Fermi surface of the organic superconductor (MDT-ST)(I$_3$)$_{0.417}$ reconstructed by incommensurate potential

Tadashi Kawamoto and Takehiko Mori

Department of Organic and Polymeric Materials, Graduate School of Science and Engineering, Tokyo Institute of Technology, O-okayama, Meguro-ku, Tokyo 152-8552, Japan

Kengo Enomoto, Takako Konoike, Taichi Terashima, and Shinya Uji

National Institute for Materials Science, Tsukuba, Ibaraki 305-0003, Japan

Ayumi Takamori, Kazuo Takimiya, and Tetsuo Otsubo

Department of Applied Chemistry, Graduate School of Engineering, Hiroshima University, Kagamiyama, Higashi-Hiroshima, Hiroshima 739-8527, Japan

The effect of incommensurate potential on Fermi surface (FS), which loses any translational symmetry in the energy bands, is investigated in the organic superconductor (MDT-ST)(I$_3$)$_{0.417}$, where MDT-ST is 5H-2-(1,3-dithiol-2-ylidene)-1,3-diselena-4,6-dithiapentalene. The observed three fundamental Shubnikov–de Haas oscillations are explained by the reconstruction with the three times of the incommensurate anion periodicity. This unambiguously verifies the *selection rule* of the reconstructing vectors in incommensurate crystals. The angular magnetoresistance oscillations show that the FS has a *p*-type staggered corrugation with two nodes in the interlayer transfer integral.

I. INTRODUCTION

For many years, the Fermi surface (FS) topologies of metals and organic conductors have been studied using techniques such as the de Haas–van Alphen (dHvA) and Shubnikov–de Haas (SdH) oscillations.[1,2] In this respect, FS under a superlattice structure is of interest because when a superlattice potential is added to the original lattice, the Brillouin zone (BZ) is reconstructed according to the new reciprocal lattice. If the periodicity of the superlattice potential is *commensurate* with the original one, it is easy to define the new BZ. For instance, the original BZ is simply halved along the a^* axis of the reciprocal lattice if the superlattice vector q is $a^*/2$. The energy bands are folded back at the new zone boundaries so that the electronic states meet the translational symmetry in the superlattice potential, which is well known as Bloch's theorem. However, when the q vector is *incommensurate*, we cannot generally define the BZ because any translational symmetry is lost.

Incommensurate potential is introduced on electronic states by density wave formation in various materials. In η-Mo$_4$O$_{11}$ and NbSe$_3$,[3,4] for instance, the electronic states are subject to incommensurate superlattice potential by charge-density wave (CDW) formation. In these materials, the SdH oscillations with very low frequencies have been observed below the CDW transition temperature, which can be ascribed to small closed orbits formed by the reconstruction of the FS's. The observed small pockets have been obtained by the FS reconstruction by the fundamental periodic vector q of the CDW. In the case of incommensurate crystals, Hg$_{3-\delta}$AsF$_6$ and Hg$_{3-\delta}$SbF$_6$, the results of the dHvA measurements have been also explained by the FS reconstruction by the fundamental periodic vector q of the incommensurate

mercury-chain sublattice.[5] The validity of such simple zone-folding procedures, which have been empirically adopted to explain the experimental results in many cases, is not trivial, because the obtained energy bands do not meet the translational symmetry of the superlattice or sublattice. This problem has not been discussed in detail because of the lack of the precise structure of the original FS's and/or too complicated FS's in these materials. In organic conductors, however, it is well known that the FS's have a very simple topology and that the band structure calculation in tight binding approximation is remarkably successful. In addition, because of high quality crystals, it is easy to observe the quantum oscillations and angular magnetoresistance oscillations (AMRO), which give us the information of the detailed FS structure.[2,6–11]

Among various organic conductors, (MDT-TSF)(AuI$_2$)$_{0.436}$ (MDT-TSF: methylenedithio-tetraselenafulvalene) has a unique structure because the non-stoichiometric content of the AuI$_2^-$ anion makes incommensurate potential on the energy band on the MDT-TSF molecules.[12,13] For this AuI$_2$ salt, the x-ray measurements show the presence of the incommensurate anion structure with nq, where n is an integer and $q=0.436a^*$. The important fact is that the observed SdH oscillations with very low frequencies are not reproduced by the empirical procedure, the simple zone folding with q, but by zone folding with the third harmonic $3q$.[14] This procedure does not meet the translational symmetry of the sublattice, either, but all the oscillations are consistently explained. We have proposed that the FS reconstruction occurs only by a single shift vector associated with the most dominant sublattice potential in an incommensurate crystal; we call it the "selection rule" of the reconstructing vectors.
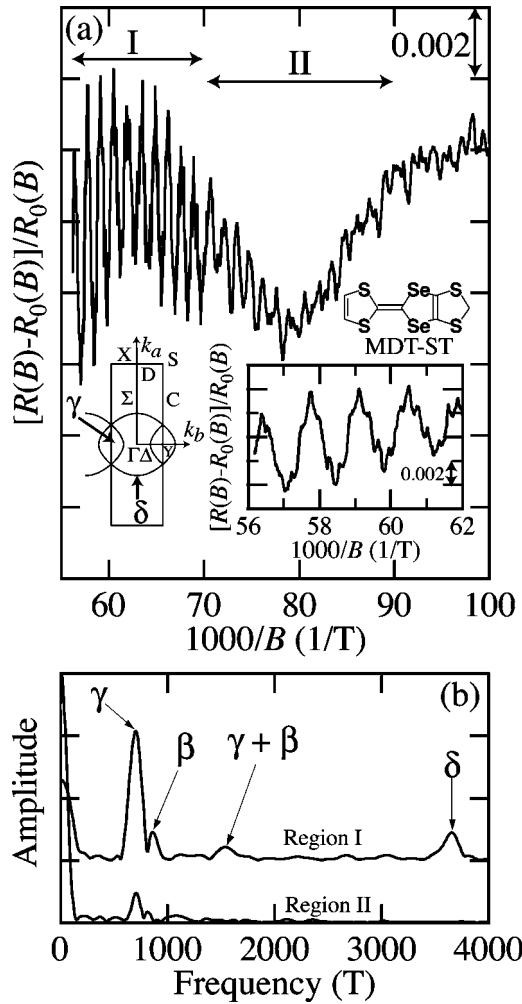
FIG. 1. (a) The SdH signal of (MDT-ST)(I$_3$)$_{0.417}$ for $B\|c$ at 35 mK. Insets are the high field region and the calculated FS without incommensurate anion lattice potential (Ref. 16). (b) The FFT spectra of the SdH oscillation in two field regions defined in (a).

When we replace half of the selenium atoms in MDT-TSF by sulfur, the resulting donor, called MDT-ST [MDT-ST: 5H-2-(1,3-dithiol-2-ylidene)-1,3-diselena-4,6-dithiapentalene depicted in Fig. 1], forms similar incommensurate organic superconductor (MDT-ST)(I$_3$)$_{0.417}$ with T_c=4.3 K.[15–17] This I$_3$ salt has a uniform donor stacking along the a axis and the donors form a conducting sheet on the (a,b) plane. The crystallographic c axis is perpendicular to the (a,b) plane, because the crystal system is orthorhombic. Our band calculation, based on the donor arrangement, gives the overlapping cylindrical FS's depicted in Fig. 1, in which the cross section of the δ orbit, $A_{F,\delta}$, is 41.7% of the first BZ whose number is equal to the amount of charge transfer coming from the anion content 0.417, and the γ orbit area, $A_{F,\gamma}$, is 8.0% of the first BZ.[16] Since the donor/anion ratio of this salt is a little different and the resulting FS overlapping is different from those of the AuI$_2$ salt, the I$_3$ salt is a good material to test the generality of the FS reconstruction rule in the incommensurate crystals.

In this paper, we present systematic investigation of the FS in (MDT-ST)(I$_3$)$_{0.417}$ with the incommensurate anion po-

tential by the SdH oscillation and AMRO. We also give a simple procedure in the reconstruction of the FS to understand the observed FS's in the SdH measurements.

II. EXPERIMENT

Single crystals were prepared by electrocrystallization.[15] For the SdH measurements, the samples were mounted on a one-axis rotator in the dilution refrigerator in a 20 T superconducting magnet. For the AMRO measurements, the samples were mounted on a two-axis rotator in a cryostat in a 14 T superconducting magnet. Both measurements were carried out by the four-probe method with ac current (200–300 μA) along the c axis, i.e., interlayer resistance R_{zz}. All magnetoresistance measurements were carried out at Tsukuba Magnet Laboratories, NIMS.

III. RESULTS AND DISCUSSION

Figure 1(a) shows the oscillatory part (SdH signal) of the resistance represented by $[R(B)-R_0(B)]/R_0(B)$, rescaled by the nonoscillatory background $R_0(B)$ at 35 mK ($B\|c$). Figure 1(b) shows the fast Fourier transformation (FFT) spectra obtained in two field regions I and II defined in Fig. 1(a). In the high field region (I), there are four peaks, which are assigned to γ, β, $\gamma+\beta$, and δ orbits later. In the low field region (II), only the γ orbit is clearly distinguished from the noise level.

The SdH signals have been analyzed in the conventional way using the Lifshitz–Kosevich (LK) formula for the FFT amplitude, A_{FFT}.[1,18] As shown in Fig. 2(a), the SdH frequencies roughly show $1/\cos\theta$ behavior expected for quasi-two-dimensional electronic systems, where θ is the angle between the magnetic field and the c axis in the (a,c) plane. The obtained frequencies are summarized in Table I, with the ratios of the cross-sectional area to the first BZ based on the donor lattice.

Temperature dependences of the oscillation amplitudes divided by temperature, called mass plots, are presented in Fig. 2(b). The solid lines are the calculated results according to the LK formula. The determined effective cyclotron mass ratios, $\mu_c=m^*/m_0$ (m_0 is the free electron mass), are listed in Table I. The effective cyclotron mass of the 1540 T orbit is not twice that of the β or γ orbit, which indicates that this orbit is neither the second harmonic of the β nor of the γ orbit, but the $\gamma+\beta$ orbit. The Dingle temperatures, T_D, simply determined from the field dependences of the oscillations, are also shown in Table I. The Dingle temperatures in Table I for γ and δ approximately give the lower and upper limits, respectively, because the γ and δ orbits are expected to include some Bragg reflection and magnetic breakdown points. Although the energy bands are degenerated on the C line owing to the donor lattice symmetry ($Pnma$), the incommensurate anion lattice along the a axis destroys this symmetry. This broken symmetry makes the δ orbit a magnetic breakdown orbit appearing only at high magnetic fields.

The oscillation amplitude of the γ orbit shows a drastic decrease at $\theta\sim30°$ [Fig. 2(c)]. This decrease is caused by the Zeeman spin splitting damping factor, $R_S=|\cos[\pi g^*\mu_c(\theta)/2]|$, for the fundamental SdH oscillation
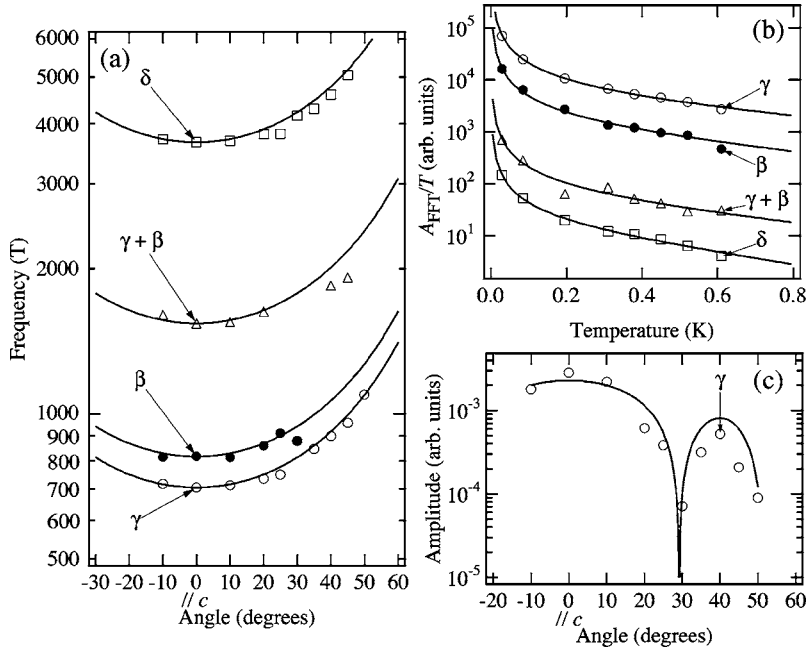
FIG. 2. (a) Angle dependences of the SdH frequencies, (b) mass plots, and (c) angle dependence of the SdH amplitude of (MDT-ST)$(I_3)_{0.417}$. The solid lines in (a) show the $1/\cos\theta$ curves, and the solid lines in (b) and (c) are the fitted results.

amplitude, where g^* is the effective conducting electron g factor renormalized by many-body effects.[1] When we assume $\mu_c(\theta) = \mu_c/\cos\theta$, substitution of this θ-dependence in R_S yields a periodic vanishing of R_S. It becomes zero every time when $g^*\mu_c/\cos\theta$ is an odd integer, a so called spin-splitting zero condition. We obtain $g^* = 1.5$ for the γ orbit from Fig. 2(c). The obtained value reduced from the free electron g factor means large renormalization by many-body effects.[2]

Figure 3(a) shows angle dependence of the magnetoresistance at 1.7 K under the field of 13.5 T. The field orientation is defined by a tilt angle θ, between the field direction and the c axis, and an azimuthal angle ϕ which is formed by the projection of the field on the (a,b) plane. This definition is shown in the inset of Fig. 3(a). Although a usual AMRO shape has a minimum at $\theta = 0°$ in a quasi-two-dimensional system, the present data have a peak at $\theta = 0°$, whose magnitude increases with increasing $|\phi|$. This peak is not observed in the AuI$_2$ salt with similar FS's.[19] Yagi and Iye have demonstrated that the $\theta = 0°$ peak appears when the FS has p-type or d_{xy}-type staggered warping.[20] The AMRO for p-type corrugation has a twofold symmetry with respect to the azimuthal angle ϕ, whereas d_{xy}-type corrugation gives a fourfold symmetrical AMRO. Moreover, they have pointed out that the $\theta = 0°$ peak intensity decreases with decreasing $|\phi|$

for p-type corrugation. The observed AMRO of the present compound in Fig. 3(a) meets the requirements of p-type corrugation. All FS's are made by the zone folding of the single energy band corresponding to the δ orbit. Therefore, it is reasonable to assume that the energy band of the δ orbit has
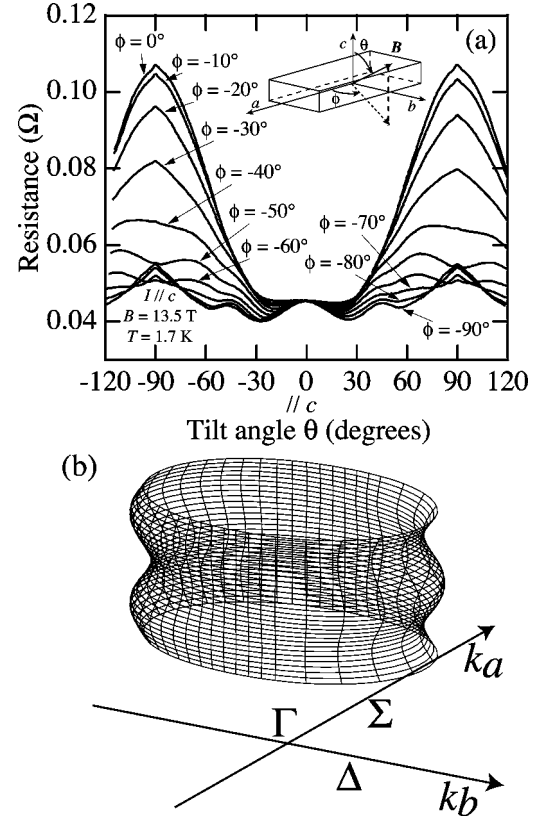

FIG. 3. (a) Angular-dependent magnetoresistance oscillations of (MDT-ST)$(I_3)_{0.417}$. (b) The p-type staggered warping FS. The magnitude of the k_c axis warping has been increased to emphasize the corrugation shape.

TABLE I. SdH frequencies, cross-sectional FS-area ratios, effective cyclotron mass ratios, and Dingle temperatures.

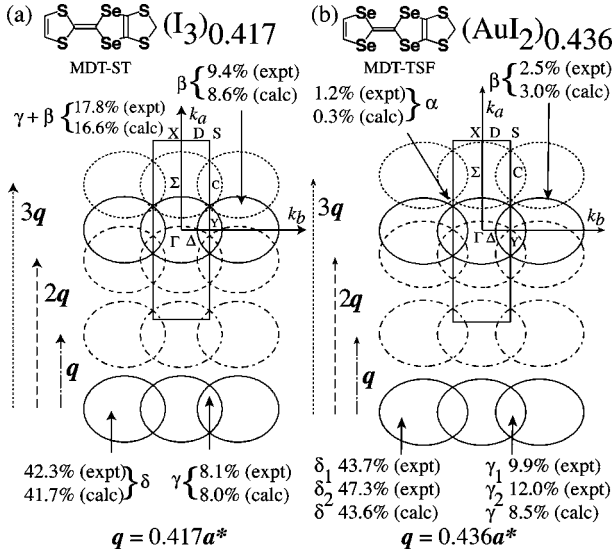| Orbit	F (T)	A_F/A_{BZ} (%)	m^*/m_0	T_D (K)
γ	704	8.14	1.7	2.4
β	816	9.44	2.1	4.0
$\gamma+\beta$	1540	17.8	2.2	4.1
δ	3660	42.3	2.9	4.4

FIG. 4. Reconstructed FS in the $k_a k_b$ plane translated by q (dash-dotted lines), $2q$ (dashed lines), and $3q$ (dotted lines) on to the original FS's (solid lines) of (a) (MDT-ST)$(I_3)_{0.417}$ and (b) (MDT-TSF)$(AuI_2)_{0.436}$. The first BZ is calculated from the donor cell.

FIG. 5. (a) The definition of the full peak width 2Δ. (b) Azimuthal angle ϕ dependence of the full peak width 2Δ. The curves represent the model prediction with $t_c/E_F = 0.032$ for three kinds of orbits. (c) Projection of the calculated FS's onto the $k_a k_b$ plane, where the line thickness means the corrugation based on $t_c/E_F = 0.032$ estimated by the 90° peak structure analysis. The reconstructed FS's by $3q$ are added.

p-type energy dispersion. The energy dispersion relation of the corrugated cylindrical FS is generally

$$E = \frac{\hbar^2}{2m_a}k_a^2 + \frac{\hbar^2}{2m_b}k_b^2 - 2t_\perp(\phi)\cos(d_\perp k_c), \quad (1)$$

where m_i is the effective mass along the k_i direction, $d_\perp$ is the effective interlayer spacing $(d_\perp = c/2 = 12.643$ Å at 18.5 K in Ref. 16), and $t_\perp(\phi)$ is the interlayer transfer integral depending on the azimuthal angle ϕ. For *p*-type warping, $t_\perp(\phi)$ is described as the following equation:[20]

$$t_\perp(\phi) = t_\perp(k_a, k_b) = \frac{k_b}{\sqrt{k_a^2 + k_b^2}} t_c, \quad (2)$$

where t_c is the constant transfer integral along the k_c direction. This formula demonstrates that the interlayer transfer integral is zero on the Σ line in the first BZ as shown in Fig. 3(b) for the fundamental FS, the δ orbit. Therefore, a field inclination at $\phi = 0°$ is least affected by the *p*-type corrugation of the FS and hence, the $\theta = 0°$ peak is minimized at this special ϕ. The $\theta = 0°$ peak is also observed for the high-T_c cuprate superconductor $Tl_2Ba_2CuO_{6+\delta}$; the feature is explained in terms of a higher order corrugation with a fourfold symmetry in the fundamental FS.[21]

In the observed FS's, two orbits, β and $\gamma + \beta$, are not explained from the band calculation. This indicates that the FS is reconstructed by the incommensurate anion potential. Although the reconstruction with vector $q = 0.417a^*$ does not make a new pocket, those with $2q$ and $3q$ lead to new closed orbits [Figs. 4(a) and 5(c)]. The $2q$ reconstruction makes several new overlapping regions, but this vector does not make the β orbit. Then the observed orbits are explained by the $3q$ reconstruction of the FS. The x-ray oscillation photograph shows that the intensity of the $3q$ spots are even stron-
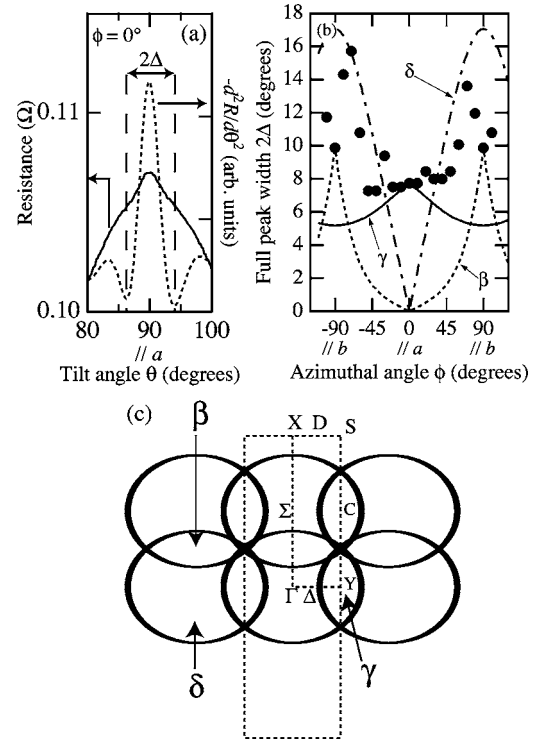
ger than the other nq spots intensity.[16] Our proposed "selection rule" requires that the shift vector of the FS should be $3q$, which is in agreement with the results of the SdH measurements. The vector $3q$ is associated with the average distance of I-I [3.1490(5) Å at 18.5 K in Ref. 16] in the real space. The Bloch theorem is not fulfilled for the electronic states in the reconstructed energy bands by $3q$, although the experimental results are quite well explained by the $3q$ reconstruction. The reason is probably as follows: The incommensurate potential is significantly small as compared with that made by the donor molecules and the conduction electrons perturbatively feel the incommensurate potential. Judging from the x-ray experiments, the dominant sublattice potential is given by $3q$ vector. This potential makes larger energy gaps in the original bands at the boundaries of the new BZ than the other higher-order sublattice potentials. In the SdH experiments, such small energy gaps formed by the higher-order potentials are not observable because of the magnetic breakdown. Therefore, our selection rule is probably validated only when the incommensurate potential is treated perturbatively. Although two new closed orbits, α and β, appear in the case of the AuI$_2$ salt [Fig. 4(b)], the α orbit vanishes and the β orbit area, $A_{F,\beta}$, becomes larger (8.6% of the first BZ) than $A_{F,\gamma}$ in the case of the I$_3$ salt [Fig. 4(a)], where we assume the FS shape of the δ orbit to be an ellipsoid with the overlapping area corresponding to the γ orbit. These results are closely associated with the difference in the

charge transfer degree between the I_3 salt and the AuI_2 salt.

Finally, we estimate the interlayer transfer integral t_c. Hanasaki *et al.* have demonstrated that the magnetoresistance peak structure for the magnetic fields nearly parallel to the conducting plane, i.e. $\theta = 90°$, we call it the $\theta = 90°$ peak, is ascribed to the closed orbits formed on the side of the corrugated two-dimensional FS.[22] McKenzie and Moses have shown that the $90°$ peak is one of the requirements for the coherency of the interlayer transport.[23] We define this full peak width, $2\Delta(\phi)$, as shown in Fig. 5(a). The present compound has a p-type corrugation FS with two warping vanishing points along the Σ line. This indicates that the $90°$ peak vanishes at $\phi = 0°$. Although the peak structure is observed for $\phi = 0°$ [Fig. 5(a)], this is originated in the γ orbit. In the present compound, the magnitude of the warping, $t_\perp$, depends on the azimuthal angle, and only $2\Delta(\phi = 0°)$ is coming from one FS, the γ orbit. We obtain $t_c/E_F = 0.032$ by

$$2\Delta(\phi = 0°) = 2k_{F,\max}^\gamma d_\perp \frac{\pi/b}{\sqrt{(\pi/b)^2 + (k_{F,\max}^\gamma)^2}} \frac{t_c}{E_F}, \quad (3)$$

where 2Δ is measured in radians and $k_{F,\max}^\gamma$ is the maximum Fermi wave number along the k_a axis of the γ orbit. We can simulate $2\Delta(\phi)$ for the i orbit $(i = \gamma, \beta, \delta)$ by the following equation under the reconstructed FS's in Fig. 4(b):

$$2\Delta(\phi) = 2k_F^i(\phi) d_\perp \frac{k_b^i}{\sqrt{(k_a^i)^2 + (k_b^i)^2}} \frac{t_c}{E_F}. \quad (4)$$

Figure 5(b) shows the calculated results under $t_c/E_F = 0.032$. Our simulation shows that in the large angle region, $|\phi| > 30°$, the peak width comes from the β and δ orbits. The obtained parameter t_c/E_F and the results of the SdH measurements give the FS's as shown in Fig. 5(c). The obtained FS's are in good agreement with the model reconstructed by $3q$.

IV. CONCLUSION

In summary, $(MDT\text{-}ST)(I_3)_{0.417}$ has three kinds of corrugated cylindrical FS's demonstrated by the SdH oscillations. The γ and δ orbits are explained from the donor arrangement, and the β orbit originates in the reconstructed FS by the strong incommensurate anion potential periodicity $3q$. The only one reconstructing vector is selected by the magnitude of the incommensurate potential; this works as the selection rule of the reconstructing vectors. This is the general FS reconstruction rule for incommensurate crystals. The AMRO with the zero degree peak indicates that the FS is a p-type staggered warping cylinder with two corrugation vanishing points along the Σ line.

[1] D. Shoenberg, *Magnetic Oscillations in Metals* (Cambridge University Press, Cambridge, 1984).

[2] J. Wosnitza, *Fermi Surfaces of Low Dimensional Organic Metals and Superconductors* (Springer, Berlin, 1996).

[3] S. Hill, S. Valfells, S. Uji, J. S. Brooks, G. J. Athas, P. Sandhu, J. Sarrao, Z. Fisk, J. Goettee, H. Aoki, and T. Terashima, Phys. Rev. B **55**, 2018 (1997).

[4] M. P. Everson, A. Johnson, H.-A. Lu, R. V. Coleman, and L. M. Falicov, Phys. Rev. B **36**, 6953 (1987).

[5] E. Batalla, F. S. Razavi, and W. R. Datars, Phys. Rev. B **25**, 2109 (1982).

[6] M. V. Kartsovnik, P. A. Kononovich, N. V. Laukhin, and I. F. Schegolev, JETP Lett. **48**, 541 (1988).

[7] K. Kajita, Y. Nishio, T. Takahashi, W. Sasaki, R. Kato, H. Kobayashi, A. Kobayashi, and Y. Iye, Solid State Commun. **70**, 1189 (1989).

[8] K. Yamaji, J. Phys. Soc. Jpn. **58**, 1520 (1989).

[9] R. Yagi, Y. Iye, T. Osada, and S. Kagoshima, J. Phys. Soc. Jpn. **59**, 3069 (1990).

[10] Y. Kurihara, J. Phys. Soc. Jpn. **61**, 975 (1992).

[11] V. G. Peschansky, J. A. Roldan Lopez, and T. G. Yao, J. Phys. I **1**, 1469 (1991).

[12] K. Takimiya, Y. Kataoka, Y. Aso, T. Otsubo, H. Fukuoka, and S. Yamanaka, Angew. Chem., Int. Ed. **40**, 1122 (2001).

[13] T. Kawamoto, T. Mori, K. Takimiya, Y. Kataoka, Y. Aso, and T. Otsubo, Phys. Rev. B **65**, 140508(R) (2002).

[14] T. Kawamoto, T. Mori, C. Terakura, T. Terashima, S. Uji, K. Takimiya, Y. Aso, and T. Otsubo, Phys. Rev. B **67**, 020508(R) (2003).

[15] K. Takimiya, A. Takamori, Y. Aso, T. Otsubo, T. Kawamoto, and T. Mori, Chem. Mater. **15**, 1225 (2003).

[16] T. Kawamoto, T. Mori, S. Uji, J. I. Yamaura, H. Kitagawa, A. Takamori, K. Takimiya, and T. Otsubo, Phys. Rev. B **71**, 172503 (2005).

[17] T. Kawamoto, T. Mori, T. Terashima, S. Uji, A. Takamori, K. Takimiya, and T. Otsubo, J. Phys. Soc. Jpn. **74**, 1529 (2005).

[18] I. M. Lifshitz and A. M. Kosevich, Sov. Phys. JETP **2**, 636 (1956).

[19] T. Kawamoto, T. Mori, C. Terakura, T. Terashima, S. Uji, H. Tajima, K. Takimiya, Y. Aso, and T. Otsubo, Eur. Phys. J. B **36**, 161 (2003).

[20] R. Yagi and Y. Iye, Solid State Commun. **89**, 275 (1994).

[21] N. E. Hussey, M. Abdel-Jawad, A. Carrington, A. P. Mackenzie, and L. Balicas, Nature (London) **425**, 814 (2003).

[22] N. Hanasaki, S. Kagoshima, T. Hasegawa, T. Osada, and N. Miura, Phys. Rev. B **57**, 1336 (1998).

[23] R. H. McKenzie and P. Moses, Phys. Rev. Lett. **81**, 4492 (1998).